



CamoVid60K: A Large-Scale Video Dataset for Moving Camouflaged Animals Understanding

Tuan-Anh Vu^{1,2} · Ziqiang Zheng¹ · Chengyang Song³ · Qing Guo^{2,4} · Ivor W. Tsang² · Sai-Kit Yeung¹

Received: 16 October 2025 / Accepted: 24 January 2026

© The Author(s), under exclusive licence to Springer Science+Business Media, LLC, part of Springer Nature 2026

Abstract

We have been witnessing remarkable success led by the power of neural networks driven by a significant scale of training data in handling various computer vision tasks. However, less attention has been paid to monitoring the camouflaged animals, the masters of hiding themselves in the background. Robust and precise segmentation of camouflaged animals is challenging even for domain experts due to their similarity to the environment. Although several efforts have been made in camouflaged animal image segmentation, to the best of our knowledge, limited work exists on camouflaged animal video understanding (CAVU). Biologists often prefer videos for monitoring and understanding animal behaviors, as videos provide redundant information and temporal consistency. However, the scarcity of labeled video data significantly hinders progress in this area. To address these challenges, we present **CamoVid60K**, a diverse, large-scale, and accurately annotated video dataset of camouflaged animals. This dataset comprises **218** videos with **62,774** finely annotated frames, covering **70** animal categories, which *surpasses* all previous datasets in terms of the number of videos/frames and species included. **CamoVid60K** also offers more diverse downstream tasks in computer vision, such as camouflaged animal classification, detection, and task-specific segmentation (semantic, referring, motion), *etc.* We have benchmarked several state-of-the-art algorithms on the proposed **CamoVid60K** dataset, and the experimental results provide valuable insights for future research directions. Our dataset serves as a novel and challenging benchmark to stimulate the development of more powerful camouflaged animal video segmentation algorithms, with substantial room for further improvement.

Keywords Moving camouflaged animal · Optical flow · Video object segmentation · Video object detection

Communicated by Urs Waldmann.

✉ Tuan-Anh Vu
tavu@connect.ust.hk

Ziqiang Zheng
zzhengaw@connect.ust.hk

Chengyang Song
songchengyang@stu.ouc.edu.cn

Qing Guo
tsingqguo@ieee.org

Ivor W. Tsang
ivor_tsang@cfar.a-star.edu.sg

Sai-Kit Yeung
saikit@ust.hk

¹ Hong Kong University of Science and Technology, Hong Kong, Hong Kong

² CFAR & IHPC, A*STAR, Singapore, Singapore

³ Ocean University of China, Qingdao, China

1 Introduction

The continuous evolution of neural networks (*e.g.*, Convolutional Neural Networks (CNNs) (He et al., 2016) and Vision Transformers (ViTs) (Dosovitskiy et al., 2020)) has provided powerful and efficient tools for visual understanding based on captured images and videos. Enhancements in both *data* and *algorithm* have led to significant progress and success in the field. Large-scale datasets (*e.g.*, COCO (Lin et al., 2014), ADE20K (Zhou et al., 2017) and Object365 (Shao et al., 2019)) with supervised annotations serve as essential stimuli for developing powerful visual perception algorithms (Xie et al., 2022) and benchmarking them to reveal future research directions. However, most existing datasets mainly contain everyday objects (*e.g.*, 80 categories in COCO). This work focuses on camouflaged animals, a less explored area of research. In addition, monitoring and understanding camou-

⁴ Nankai University, Tianjin, China

flaged animals is crucial for biodiversity conservation (Soofi et al., 2022; Rands et al., 2010), as it helps protect species that are otherwise difficult to detect and are at risk of unnoticed population declines. Furthermore, studying camouflaged animals provides insights into evolutionary biology and adaptation mechanisms, enriching our scientific understanding of natural selection.

However, unlike everyday objects, collecting images and videos of camouflaged animals is more challenging, and annotation procedures usually involve domain experts. *Segmentation*, which involves generating precise masks for objects of interest, is a fundamental task in computer vision. Camouflaged animal segmentation helps accurately identify and isolate these animals from their backgrounds in images, facilitating detailed study and analysis. The resulting masks aid in gathering precise data on their behavior, habitat, and population dynamics, enhancing our overall understanding of their ecology (Lv et al., 2021; Troscianko et al., 2017). Recently, several efforts Xie et al. (2022); Cheng et al. (2022); Lamdouar et al. (2023); Vu et al. (2023) have been made to perform camouflaged animal segmentation. Specifically, camouflage is a powerful biological mechanism for avoiding detection and identification, making it more challenging to achieve precise segmentation.

Various datasets (e.g., CAMO-COCO Le et al. (2019), COD10K Fan et al. (2022), CAM-LDR Lv et al. (2023), S-COD He et al. (2023)) have been collected for image-level camouflaged animal segmentation. However, image-level camouflaged animal segmentation cannot fully satisfy biological monitoring and surveying purposes, where the activity and behavior (Yang et al., 2021) should be recorded. For video level, the MoCA dataset Lamdouar et al. (2020) is the most extensive compilation of videos featuring camouflaged objects, yet it only provides detection labels. We argue that bounding box annotations alone cannot adequately delineate camouflaged animals, especially those with irregular boundaries, poses, and patterns (e.g., the transparent fins of fish). Furthermore, despite the shift from images to videos, the data annotations remain insufficient in both volume and accuracy for developing a reliable video understanding model capable of effectively handling complex camouflaged situations.

To fill this gap and advance camouflaged animal video understanding (CAVU) in real-world scenarios, we present **CamoVid60K**, a comprehensive video dataset dedicated to studying camouflaged animals. It comprises **218** videos with **62,774** finely annotated frames, covering **70** animal categories. Table 1 compares our proposed dataset with previous ones (CAD (Pia Bideau, 2016), MoCA (Lamdouar et al., 2020), MoCA-Mask (Cheng et al., 2022), MVK (Truong et al., 2023), WATB Wang et al. (2022), and Animal-Track Zhang et al. (2022)), showing that **CamoVid60K** surpasses all previous datasets in terms of the number of videos, frames, and species included. Unlike previous

datasets that annotated every 5 frames, our dataset offers annotations for every single frame. Additionally, we provide a wider variety of annotation types (animal categories, bounding boxes, annotated masks, pseudo-label optical flow, referring expressions), making it a more effective benchmark for CAVU tasks. Our dataset supports a broad range of downstream tasks, as shown in Figure 1, including classification, detection, segmentation (semantic, referring, motion), and optical flow estimation, etc.

We propose baselines for each task and corresponding benchmarks to explore the capabilities of advanced algorithms in performing robust and precise video understanding. Our **CamoVid60K** serves as a novel and important testing set for both the computer vision and wildlife research communities.

Our main contributions are summarized as follows:

- We present a **large-scale** and **comprehensive** video dataset dedicated to the understanding of camouflaged animals, featuring **significantly more** data and annotation types than existing datasets.
- We propose a **simple pipeline** for camouflaged animal detection and segmentation that achieves performance comparable to state-of-the-art methods.
- We benchmark **various** camouflaged animal video understanding tasks, including image classification, object detection, and motion segmentation using several state-of-the-art models.

2 Related Works

2.1 Camouflaged Scene Understanding

Camouflaged scene understanding (CSU) is a hot computer vision topic aiming to learn discriminative features that can be used to discern camouflaged target objects from their surroundings (Fan et al., 2023). CSU tasks can be divided into image-level and video-level categories. Image-level CSU tasks include five main types: camouflaged object counting (Sun et al., 2023), camouflaged object localization (Lv et al., 2021, 2023), camouflaged object segmentation (Ji et al., 2023; He et al., 2023; Fan et al., 2022), camouflaged instance ranking (Lv et al., 2021, 2023), and camouflaged instance segmentation (Le et al., 2021; Pei et al., 2022). These tasks can be further categorized based on their semantic focus: object-level and instance-level. Object-level tasks focus on identifying objects, while instance-level tasks aim to differentiate various entities. Additionally, camouflaged object counting is considered a sparse prediction task due to its nature, while the other tasks are classified as dense prediction tasks. In addition, CSU video-level tasks include video camouflaged object segmentation (Ji et al., 2014; Cheng et

135 al., 2022; Xie et al., 2019) and video camouflaged object
 136 detection (Kowal et al., 2022; Lamdouar et al., 2020; Meunier et al., 2022; Lamdouar et al., 2021; Xie et al., 2022;
 137 Yang et al., 2021). Overall, the progress of video-level CSU
 138 has been somewhat slower than image-level CSU, primarily
 139 because the process of collecting and labeling video data is
 140 labor-intensive and time-consuming.
 141

142 **2.2 Video Camouflaged Object Detection and**
 143 **Segmentation**

144 We review two kinds of perception tasks for camouflaged ani-
 145 mal videos: detection (Kowal et al., 2022; Lamdouar et al.,
 146 2020; Meunier et al., 2022; Lamdouar et al., 2021; Xie et al.,
 147 2022; Yang et al., 2021) and segmentation (Lamdouar et al.,
 148 2023; Ji et al., 2014; Cheng et al., 2022; Xie et al., 2019). The
 149 former video camouflaged object detection (VCOD) yields
 150 bounding box sequences for the camouflaged animals, while
 151 the latter video camouflaged object segmentation (VCOS)
 152 generates dense pixel-level masks. MoCA Lamdouar et al.
 153 (2020) proposed the first large-scale moving camouflaged
 154 animals video dataset, featuring bounding box annotations
 155 and additional optical flows to enhance the detection of
 156 camouflaged animals. Further work Lamdouar et al. (2021)
 157 incorporated visual appearance from a static scene as addi-
 158 tional clues to promote the ability of the model to detect
 159 camouflaged animals. However, the bounding box annota-
 160 tions could not accurately describe camouflaged objects’
 161 pose, appearance, and patterns. To address this issue, Xie Xie
 162 et al. (2019) proposed a novel pixel-trajectory RNN to cluster
 163 foreground pixels and generate dense segmentation masks for
 164 object discovery in videos. MoCA-Mask Cheng et al. (2022)
 165 proposed the first large-scale dataset and benchmark with
 166 pixel-level handcrafted ground truth masks for camouflaged
 167 animal videos. However, MoCA-Mask provides bounding
 168 boxes and pixel-wise masks for **only every 5 frames**, total-
 169 ing just 4,691 frames, which is insufficient for deep learning
 170 approaches. In contrast, our dataset offers annotations for
 171 **every frame**, resulting in 62,774 annotated frames (**13 times**
 172 **larger**). This substantial increase can significantly enhance
 173 the performance of various downstream tasks. Our dataset
 174 and benchmark pave the way for future exploration and a
 175 deeper understanding of camouflaged animal analysis.

176 **3 CamoVid60K Dataset**

177 Collecting video datasets of camouflaged animals is quite
 178 challenging, even without focusing on long-form videos.
 179 Manually collecting, observing, and annotating videos with
 180 multiple annotation types is labor-intensive, time-consuming,
 181 and expensive. In addition to these costs, ensuring visual
 182 data diversity and high-quality annotations adds to the dif-

Table 1 Comparison with existing video animal datasets. Class.: Classification Label, B.Box: Bounding Box, Motion: Motion of Animal, Pseudo-label Optical Flow, Express.: Referring Expression. The frequency of annotations refers to how often each frame is annotated. For instance, MoCA-Mask provides annotations for **every 5 frames**, resulting in only 4,691 annotated frames out of a total of 22,939 frames. In contrast, our CamoVid60K dataset offers a significantly larger volume of data with more frequent annotations and a wider variety of annotation types. * *Note that*, MVK Truong et al. (2023) dataset mostly consists of *normal* marine animals with only some camouflaged animals.

Dataset	Venue	# videos / frames	# species	Frequency	Class.	B.Box	Mask	Motion	PseudoOF	Express.
CAD	ECCV’16	9 / 839	6	every 5 frames	✓		✓			
MoCA	ACCV’20	141 / 37,250	67	every frames	✓	✓		✓		
MoCA-Mask	CVPR’22	87 / 22,939	44	every 5 frames	✓		✓			
MVK*	MMM’23	1379 / ~ 992,880	-	every 30 frames	✓					✓
WATB	IJCV’23	206 / ~ 203,000	-	every frames	✓					
AnimalTrack	IJCV’23	58 / ~ 247,000	-	every frames	✓	✓				
CamoVid60K	-	218 / 62,774	70	every frames	✓	✓	✓	✓	✓	✓

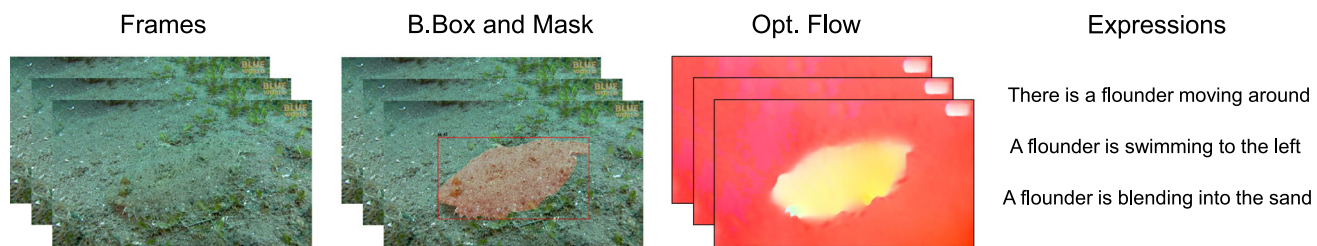


Fig. 1 Example from our proposed CamoVid60K dataset with bounding box, mask, pseudo-label optical flow, and referring expressions

183 ficulty. In this section, we propose a staged data collection
 184 and processing pipeline, as shown in Figure 2. Associated
 185 datasheets (Gebru et al., 2021) and data cards (Pushkarna
 186 et al., 2022) for our CamoVid60K dataset are provided
 187 in Appendix A.

188 3.1 Data Construction and Processing

189 3.1.1 Data Sources and Pre-Processing

190 We built our dataset by incorporating previous published
 191 datasets (Camouflaged Animals Dataset (CAD) (Pia Bideau,
 192 2016), Moving Camouflaged Animals (MoCA) (Lamdouar
 193 et al., 2020), MoCA-Mask (Cheng et al., 2022), Marine Video
 194 Kit (MVK) (Truong et al., 2023)) and crawling additional
 195 videos from the internet to cover a variety of camouflaged
 196 animals.

197 The CAD dataset includes nine short video sequences
 198 obtained from YouTube videos. Hand-labeled ground truth
 199 masks are provided for every 5 frames.

200 The MoCA dataset comprises approximately 37,000
 201 frames extracted from 141 YouTube video sequences. Most
 202 videos are presented at an image resolution of 1280 × 720
 203 and 3840 × 2160 pixels, and the videos have a frame rate
 204 of 24 FPS. This dataset includes 67 distinct species of ani-
 205 mals in locomotion within their native habitats, although it
 206 contains a few instances of animals with less camouflaged
 207 characteristics.

208 The MoCA-Mask dataset is built upon the MoCA dataset.
 209 This new subset consists of 87 video sequences with 22,939
 210 frames. It offers human-labeled segmentation masks for
 211 every 5 frames. Consequently, the ground truth (GT) is avail-
 212 able in two formats: 4,691 bounding box annotations and
 213 4,691 pixel-level masks.

214 The MVK dataset comprises 1,379 underwater videos
 215 recorded at 36 unique geographical sites during various
 216 seasons. These videos exhibit a broad duration spectrum,
 217 ranging from as short as 2 seconds to almost 5 minutes,
 218 with a total duration slightly above 12 hours. On average,
 219 the videos are roughly 29.9 seconds long, with a median
 220 length of around 25.4 seconds. Notably, the dataset presents

221 videos recorded under different conditions, such as variable
 222 light levels, points of view, water clarity, and environmen-
 223 tal conditions. They also offer approximately 40,000 frames
 224 (extracted at one FPS or every 30 frames) with associated
 225 referring expression annotations.

226 To crawl videos from the internet, we curated a list of ani-
 227 mal names that potentially have camouflage abilities. We then
 228 created a template for searching and downloading videos:
 229 “video of camouflaged/concealed + animal’s name”. By
 230 combining these with the videos from the above datasets, we
 231 initially collected 1,929 videos. We then manually checked
 232 and filtered out any blurry or irrelevant videos, retaining those
 233 with clear depictions of animals. Next, we extracted every
 234 frame of each video (instead of every 5 frames as proposed
 235 in existing datasets, see Table 1) before annotating them. At
 236 the end, our dataset comprises 218 videos with 62,774 frames
 237 of 70 animal species.

238 3.1.2 Bounding Box and Mask Annotation.

239 We utilized the annotation tool from (Zheng et al., 2023),
 240 which is heavily based on the Segment Anything Model
 241 (SAM) (Kirillov et al., 2023) for mask initialization and
 242 bounding box creation, and XMem (Cheng & Schwing,
 243 2022) for mask and bounding box propagation. We then man-
 244 ually checked and refined every frame to provide accurate
 245 bounding boxes and segmentation masks. In addition, we
 246 adopted the perceptual camouflage score (S_p) from (Lam-
 247 douar et al., 2023) to quantify the effectiveness of animals’
 248 camouflage, *i.e.*, how successfully an animal blends into
 249 its background. Based on the perceptual camouflage score,
 250 we retained videos with a score higher than the threshold
 251 ($S_p > 0.5$). Below, we explain how to compute the percep-
 252 tual camouflage score S_p :

$$253 S_p = (1 - \alpha)S_{\mathcal{R}} + \alpha S_{\mathcal{B}} \tag{1}$$

254 where $S_{\mathcal{R}}$ is the reconstruction fidelity score, $S_{\mathcal{B}}$ is the
 255 boundary score, and α is the weighting parameter.

256 In detail, given an image \mathcal{I} and a segmentation mask m_S ,
 257 the reconstruction fidelity score $S_{\mathcal{R}}$ is computed by assessing
 258 the difference between the foreground region and its recon-
 259 struction. Specifically, it counts the number of foreground

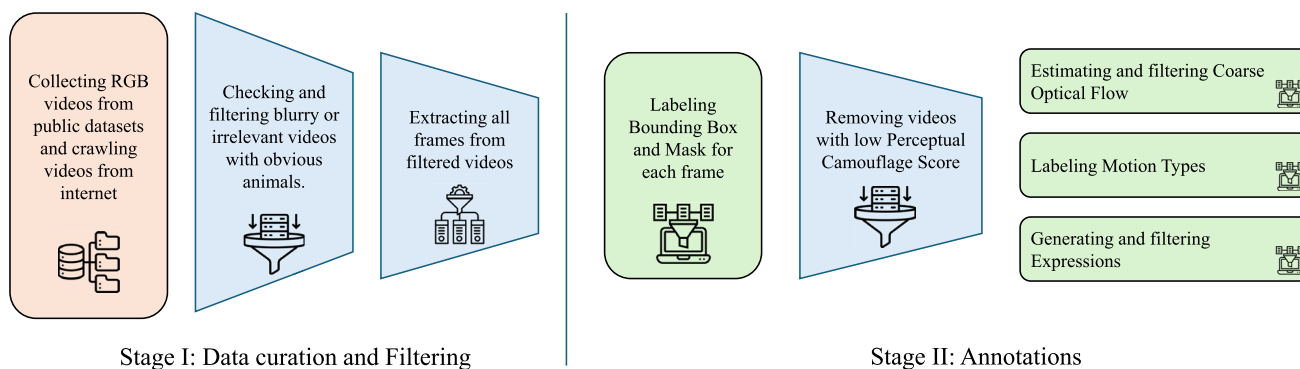


Fig. 2 CamoVid60K data pipeline. Stage I includes data curation, filtering irrelevant videos, and extracting all frames. Stage II includes data annotation, generation, and filtering

pixels ($\mathcal{I}_{fg} = \mathcal{I} \odot \text{erode}(m_S)$) that have been successfully reconstructed from the background ($\mathcal{I}_{bg} = \mathcal{I} \odot (1 - \text{dilate}(m_S))$):

$$S_{\mathcal{R}}(\mathcal{I}, m_S) = \frac{1}{N_{fg}} \sum_{(i,j) \in \mathcal{I}_{fg}} \mathcal{R}(i, j), \tag{2}$$

$$\mathcal{R}(i, j) = \begin{cases} 1, & \text{if } \|\mathcal{I}_{fg}(i, j) - \Psi_{\mathcal{I}_{bg}}(\mathcal{I}_{fg}(i, j))\|_2 < \lambda \|\mathcal{I}_{fg}(i, j)\|_2, \\ 0, & \text{otherwise,} \end{cases} \tag{3}$$

where $\Psi_{\mathcal{I}_{bg}}(\cdot)$ denotes the reconstruction operation, $N_{fg} = |\text{erode}(m_S)|$ is the total number of pixels in the foreground region, and λ is a threshold.

Then, the boundary visibility score $S_{\mathcal{B}}$ aims to measure the animal’s boundary properties (or contour visibility) by penalizing the boundary pixels that are predicted as contours in both the image’s contour (\mathcal{C}) and the ground truth animal’s contour (\mathcal{C}_{gt}) using the F1 metric:

$$S_{\mathcal{B}}(\mathcal{I}, m_S) = 1 - \text{F1}(m_b \odot \mathcal{C}_{gt}, m_b \odot \mathcal{C}), \tag{4}$$

where $m_b = \text{dilate}(m_S) - \text{erode}(m_S)$.

We used the same parameter values as in (Lamdouar et al., 2023), specifically $\alpha = 0.35$ and $\lambda = 0.2$. In addition, we illustrate the difference between low-ranking and high-ranking camouflage in Figure 3 and Figure 4.

Note that, due to the nature and characteristics of camouflaged animals and also the low resolution of videos, some frames or videos may contain errors or mislabeling at the boundaries between animals and the background. We will continue improving the quality of the mask annotations and also provide rotated bounding boxes (RBbox) in the next version. RBbox excels over traditional axis-aligned bounding boxes in three main areas: better localization (accurate fit for elongated and rotated objects), reduced overlap of different objects or instances, and improved isolation of objects

(capturing the proper aspect ratio and containing fewer background pixels).

3.1.3 Pseudo-label Optical Flow Annotation.

Previous optical flow datasets, such as Flying Chairs (Dosovitskiy et al., 2015), KITTI (Menze & Geiger, 2015), Sintel (Butler et al., 2012), and FlyingThings3D (Mayer et al., 2016), utilized either simulation software or real images with additional heavy sensor information (depth, LiDAR, etc.) and algorithms to create optical flow ground truth. This process is time-consuming and requires significant effort. Recently, with the development of deep learning techniques, many methods (Wang et al., 2023; Teed & Deng, 2020) can produce accurately estimated optical flow. Therefore, we utilized these methods for our pseudo-label optical flow annotation, using the algorithm shown in Algorithm 1. We used the pre-trained model of RAFT on FlyingThings3D (Mayer et al., 2016) and the pre-trained DINO model of ViT-B architecture.

Note that, even though our processing pipeline for optical flow annotation produces relatively accurate and dense optical flow, it is still **estimated** optical flow. Therefore, we provide pseudo-flow **as an auxiliary motion cue** (e.g., as additional input to motion segmentation) rather than as ground-truth supervision, and we **do not** use pseudo-flow as the target for any primary benchmark evaluation. Instead, all benchmark metrics reported in this paper are computed against **human annotations** (e.g., masks/boxes/motion labels) following our evaluation protocol.

3.1.4 Motion Annotation.

Following Lamdouar et al. (2020), we manually labeled our dataset according to the types of motion, as shown below. Based on these motion types, we can further annotate the camouflage methods of animals (concealing coloration, disruptive coloration, disguise, mimicry, transparency, and

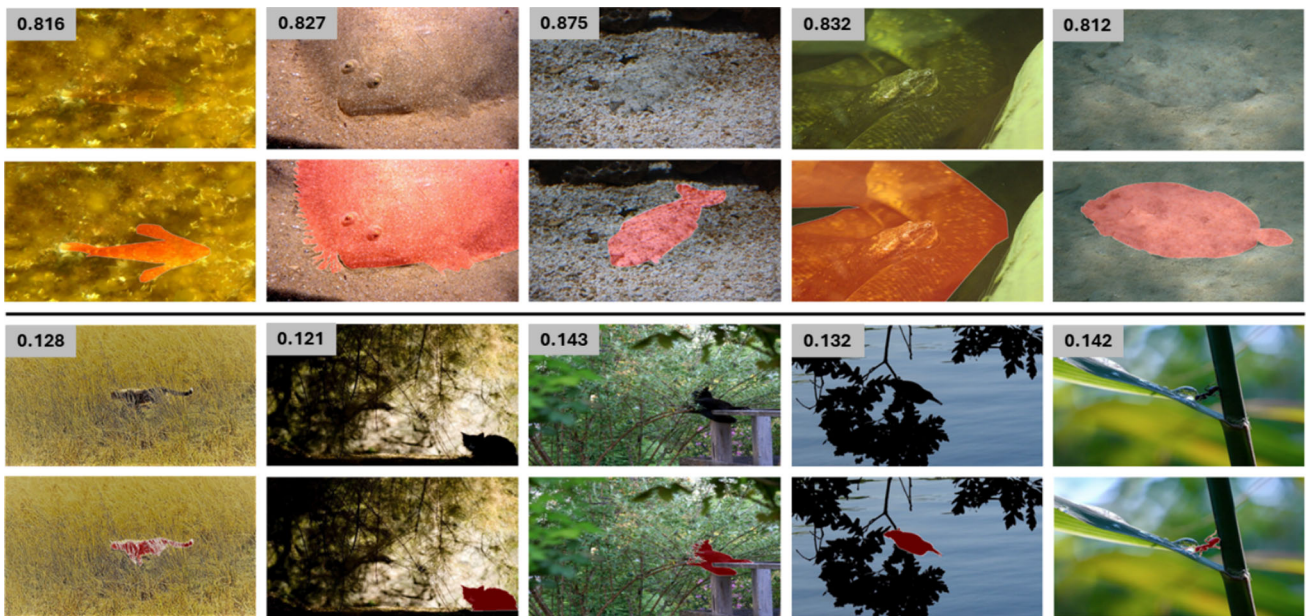


Fig. 3 The example of low-ranking and high-ranking camouflage of a single frame

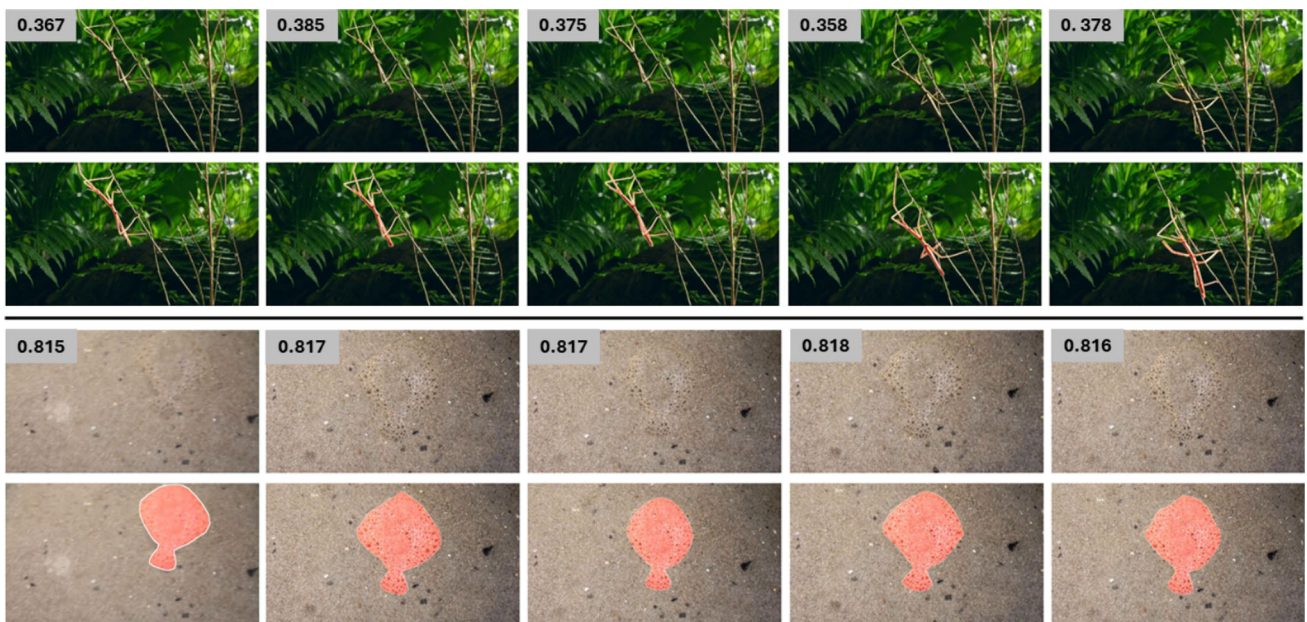


Fig. 4 The example of low-ranking and high-ranking camouflage of consecutive frames

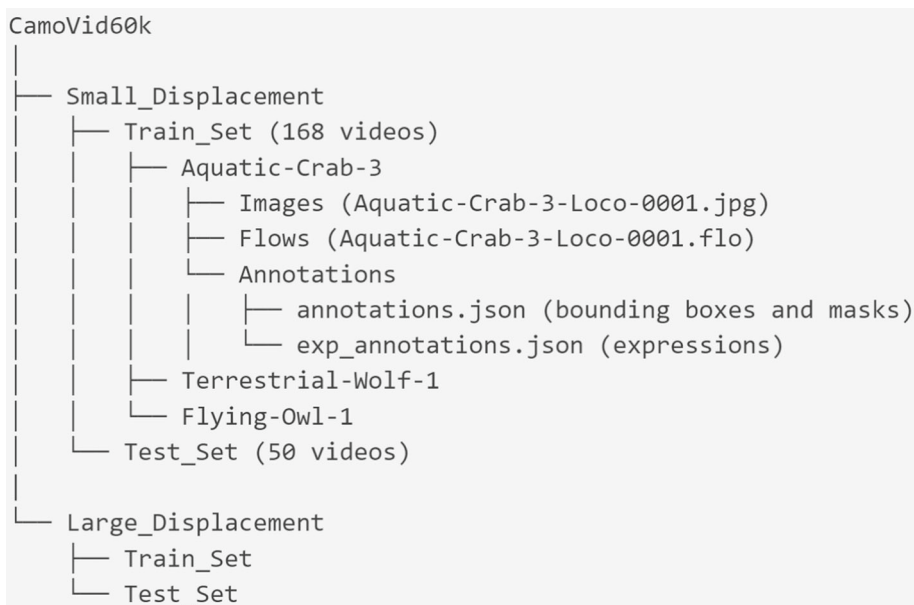
323 counter-shading), which we plan to provide in the next ver-
324 sion.

- 325 • *Locomotion*: when the animal makes movements that sig-
326 nificantly change its location.
- 327 • *Deformation*: when the animal engages in more subtle
328 movements that only change its pose while remaining in
329 the same location.
- 330 • *Still*: when the animal remains stationary.

3.1.5 Referring Expression Annotation.

331 Referring expression annotations are used for the Refer-
332 ring Video Object Segmentation (RVOS) task. RVOS differs
333 from traditional Video Object Segmentation (VOS), where
334 a mask is provided for the first frame, and the model
335 predicts the segmentation for the remaining video frames. In
336 RVOS, the initial frame mask is replaced with a referring
337 expression (*i.e.* a sentence) that accurately describes the target
338 object throughout the entire video, *e.g.* “the yellow fish swim-
339

Fig. 5 Data organization of our dataset. It includes a small and a large displacement subset



Algorithm 1 Optical Flow Computation and Filtering

- Require:** Sequence of frames
Ensure: Sequence of computed optical flows
- 1: **for** each pair of frames (i, j) **do**
 - 2: Compute all pairwise optical flows using RAFT (Teed & Deng, 2020)
 - 3: Compute DINO features (Oquab et al., 2024; Caron et al., 2021) for each frame
 - 4: Filter flows using cycle consistency and appearance consistency check
 - 5: Apply chain cycle consistent correspondences to create denser correspondences
 - 6: **end for**

ranked the candidates based on their relevance and utility for RVOS. The ranking criteria emphasized (i) correctness with respect to the target object, and (ii) discriminativeness via spatiotemporal cues, such as the target’s relative position (e.g., moving left/right or up/down) and motion pattern (e.g., swimming, approaching, blending into the background). We then selected the final three expressions per video by taking the top-ranked candidates agreed upon by both validators (e.g., overlapping selections such as #1/#3/#4 from two ranked lists). Finally, we refined the selected expressions to improve clarity and directness (e.g., resolving ambiguous references and adding the object category name when identifiable) to reduce linguistic ambiguity, given the additional difficulty posed by camouflaged targets. Video instances whose targets could not be reliably localized using language were removed from the referring-expression subset.

3.2 Dataset Specifications and Statistics

3.2.1 Data Organization.

As shown in Figure 5, we split our dataset into two subsets based on the degree of displacement between frames: small displacement (every single frame) and large displacement (every 5 frames). This division is beneficial for evaluating motion segmentation methods, as it provides a robust framework for analyzing algorithms’ performance under varying motion and displacement conditions. Each subset includes training and testing sets with images, pre-computed optical flows, and annotations. Importantly, the train/test split is performed at the **video level** to prevent data leakage. Specifically, our dataset contains **218 videos** in total, partitioned into **168 videos** for training and **50 videos** for testing, and

340 *ming toward the camera.*” This approach also differs from
 341 Referring Image Segmentation (RIS), which uses different
 342 referring expressions for each image. Referring expression
 343 annotations can be utilized for various video understanding
 344 tasks, such as RVOS (Seo et al., 2020; Yang et al., 2024),
 345 video retrieval systems with semantic understanding (Ha et
 346 al., 2023), video grounding (Mu et al., 2024), etc.

347 To generate referring expressions, we first employed GPT-
 348 4V (xxxx, 2023) to produce concise captions (within 30
 349 words) describing the target object for each frame. We
 350 observed reduced caption accuracy for aquatic animals;
 351 therefore, for aquatic videos, we used MarineGPT (Zheng
 352 et al., 2023), a vision-language model designed for the
 353 marine domain, to generate the initial captions. From these
 354 frame-level captions, we formed multiple candidate refer-
 355 ring expressions for each video sequence and then applied a
 356 human verification and refinement process to obtain the final
 357 annotations.

358 Specifically, two validators were presented with each
 359 video and its candidate expressions, and independently

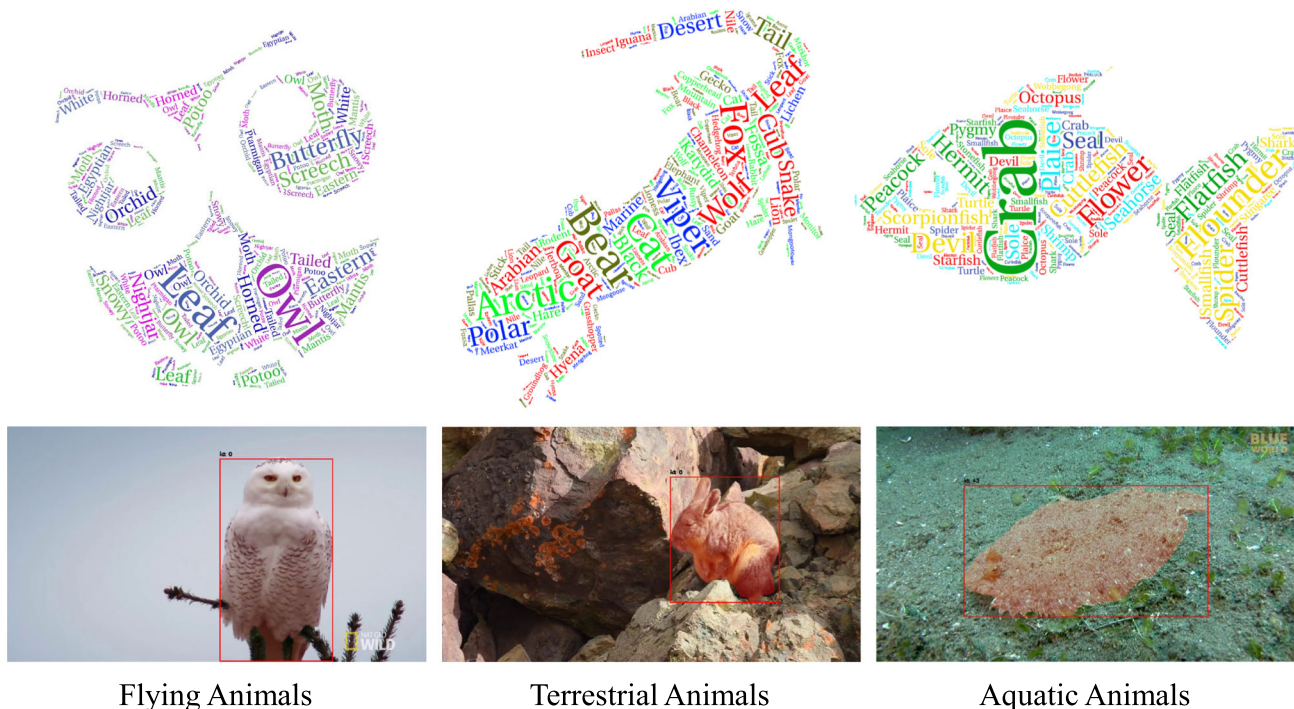


Fig. 7 Word cloud of category distribution of camouflaged animals with corresponding examples showing bounding box, segmentation mask (bottom)

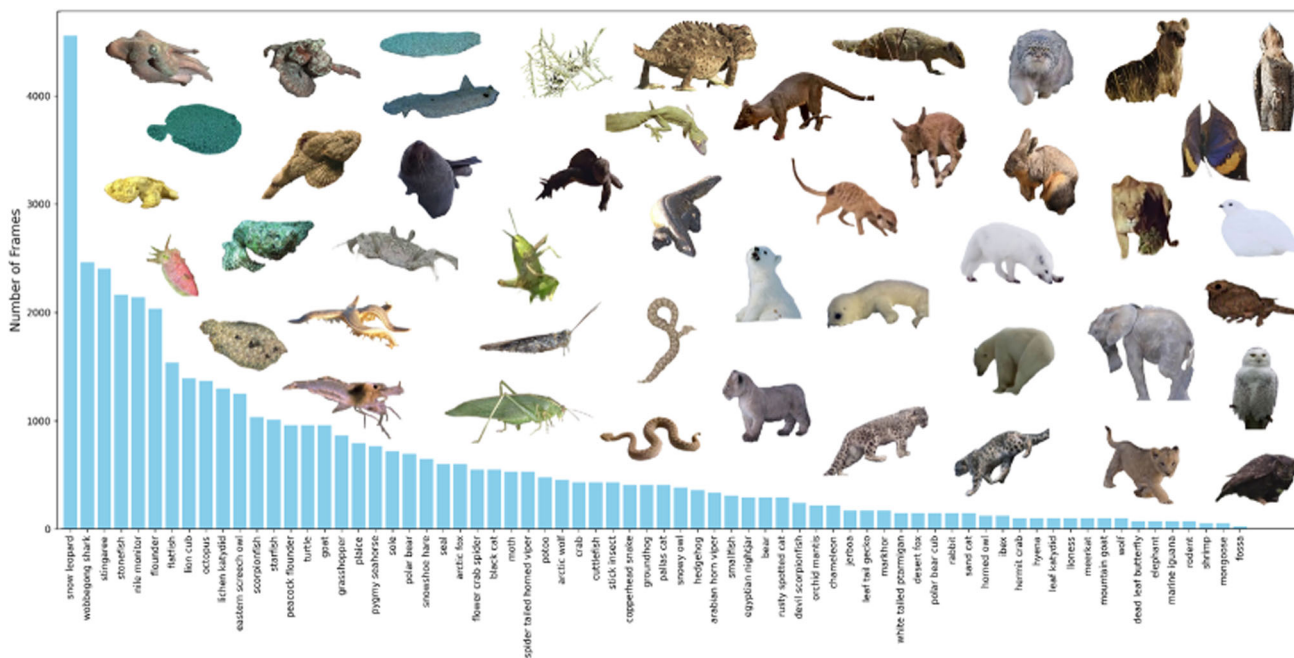


Fig. 8 Category distribution (ranging from 100 to 4,500 frames) and some visual examples (extracted animal masks) of our dataset. The variety ensures a wide range of camouflaged animals, allowing for comprehensive evaluation across various scenarios

433 2014), mean Intersection Over Union (mIoU), mean Dice
434 (mDic).

- 435 • *Object Detection*: we use the mean Average Precision
436 (mAP).
- 437 • *Image Classification*: we use the mean Accuracy (mAcc).
- 438 • *Referring Segmentation*: we utilize the mIoU, region sim-
439 ilarity \mathcal{J} and contour accuracy \mathcal{F} , and their average
440 $\mathcal{J}\&\mathcal{F}$ for video object segmentation.

41 4 A simple pipeline to discern camouflaged 42 animals

443 After constructing the dataset, we propose a simple pipeline
444 based on the Mask2Former architecture (Lamdouar et al.,
445 2023; Cheng et al., 2022) for both object detection and motion
446 segmentation tasks. The goal of this baseline is to provide a
447 **transparent starting point** and a consistent implementation
448 for benchmarking on CamoVid60K, rather than to propose
449 a heavily engineered state-of-the-art model. In our case, we
450 directly use the refined optical flow provided in our dataset
451 instead of utilizing the RAFT method (Teed & Deng, 2020) to
452 estimate raw optical flow, as done in (Lamdouar et al., 2023).
453 The images and associated estimated flows are passed into
454 two separate encoders for feature extraction. Subsequently,
455 the image and flow features at each timestamp are aggregated
456 before being fed into the decoder to predict the segmenta-
457 tion mask. While this design is intentionally lightweight,
458 an important direction for future work is to replace pre-
459 computed flow with learnable motion representations trained
460 end-to-end, which may further improve both practicality and
461 performance.

462 4.1 Visual Encoder.

463 We adopt the SInet-v2 (Fan et al., 2022) architecture, which
464 takes an RGB sequence as input $I^v = \{I_1^v, I_2^v, \dots, I_n^v\} \in$
465 $\mathbb{R}^{n \times d_v \times h \times w}$, where n is the number of frames, d_v is the
466 dimension of each frame, and h and w are the height and
467 width, respectively. The visual encoder outputs visual fea-
468 tures $\{f_1^v, f_2^v, \dots, f_n^v\} = \Phi_{\text{visual}}(I^v)$.

469 4.2 Motion Encoder.

470 Inspired by the motion segmentation architecture (Lamdouar
471 et al., 2021), we use a lightweight ConvNet that takes as
472 input a sequence of optical flows $I^f = \{I_1^f, I_2^f, \dots, I_n^f\} \in$
473 $\mathbb{R}^{n \times d_f \times h \times w}$, where d_f is the dimension of the flow field, and
474 outputs motion features $\{f_1^m, f_2^m, \dots, f_n^m\} = \Phi_{\text{motion}}(I^f)$.
475 We then concatenate the motion features with learned spa-
476 tial and temporal positional encodings to produce a set of
477 enriched motion features.

478 4.3 Decoder.

479 We adopt the Mask2Former (Cheng et al., 2022) architec-
480 ture, which includes Transformer and Pixel decoders. The
481 Transformer decoder combines a trainable query for mask
482 embedding with the outputs of the motion encoder and visual
483 features. Similar to Mask2Former, this query attends to multi-
484 scale motion features and visual features, resulting in mask
485 embedding for the moving object. Additionally, similar to the
486 pixel decoder in Mask2Former, a ConvNet decoder with low
487 computational complexity uses skip connections to gener-
488 ate high-resolution segmentation masks and bounding boxes
489 from the motion features and mask embedding.

490 4.4 Training and Loss.

491 To optimize our pipeline, we utilize the L1 loss for bounding
492 box regression, cross-entropy loss for the confidence score,
493 and binary cross-entropy (BCE) loss for motion segmenta-
494 tion. The total loss for training our pipeline is defined as
495 follows:

$$496 \mathcal{L} = \mathcal{L}_{\text{BCE}} + \mathcal{L}_{\text{L1}} + \mathcal{L}_{\text{CE}}, \tag{5}$$

497 where \mathcal{L}_{BCE} is the binary cross-entropy loss for motion seg-
498 mentation, \mathcal{L}_{L1} is the L1 loss for bounding box regression,
499 and \mathcal{L}_{CE} is the cross-entropy loss for the confidence score.

500 5 Experiments

501 This section introduces the baselines and training details
502 for each task. We thoroughly analyze each task in our
503 experiments and discuss the effectiveness of each method,
504 including ours.

505 5.1 Baselines

506 **For the motion segmentation task**, we selected recent
507 state-of-the-art (SOTA) methods for comparison, including
508 two frame-based methods (PraNet (Fan et al., 2020) and
509 SInet-v2 (Fan et al., 2022)) and two video-based methods
510 (MG (Yang et al., 2021) and SLT-Net (Cheng et al., 2022)).
511 For a fair comparison, we utilized the implementations pro-
512 vided by the authors and trained all methods using the same
513 training set.

514 **For the object detection task**, we compared our approach
515 with three well-known detection methods: Faster R-CNN (Ren
516 et al., 2015), DETR (Carion et al., 2020), and DINO (Zhang
517 et al., 2023). We followed the $1 \times$ (12-epoch) training setting
518 and used the same ResNet50 (He et al., 2016) backbone for
519 all methods.

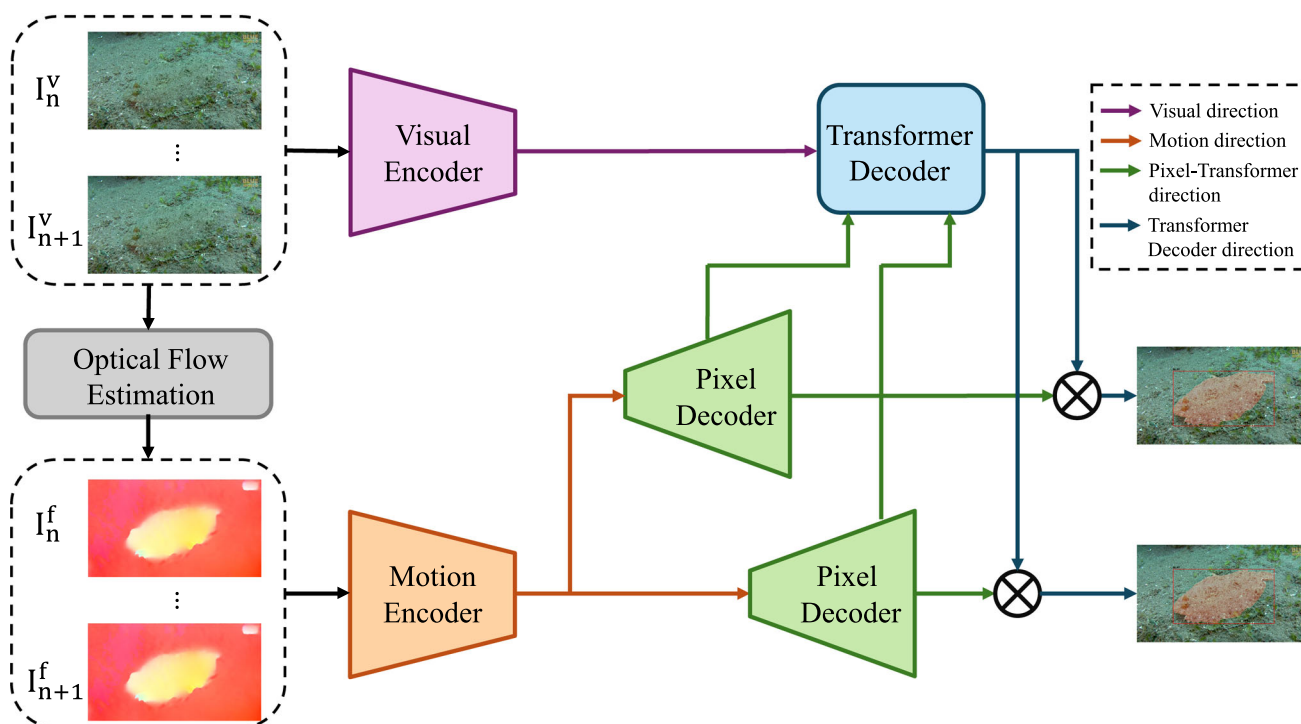


Fig. 9 Our simple pipeline takes a sequence of images (or a video) and the associated pre-computed optical flow (provided in our dataset) as input. They are fed into separate encoders for feature extraction. Then, the motion features with spatial and temporal positional encoding are

passed to Pixel Decoders to produce a set of enriched motion features. Next, the Transformer Decoder takes the visual features and enriched motion features to produce mask embedding for the moving object and bounding box

Table 2 Quantitative results of motion segmentation on our CamoVid60K dataset. Our simple pipeline achieves performance comparable to that of other SOTAs on certain metrics.

Methods		$S_\alpha \uparrow$	$F_\beta^w \uparrow$	$E_\phi \uparrow$	$MAE \downarrow$	mDice \uparrow	mIoU \uparrow
Image-based	PraNet (Fan et al., 2020)	0.526	0.161	0.547	0.045	0.198	0.144
	SINet-v2 (Fan et al., 2022)	0.529	0.166	0.553	0.042	0.206	0.149
	FSEL (Sun et al., 2024)	0.542	0.184	0.565	0.048	0.213	0.154
	Ours (RGB-only)	0.536	0.178	0.557	0.046	0.206	0.151
Video-based	MG (Yang et al., 2021)	0.522	0.153	0.541	0.043	0.197	0.141
	SLT-Net (Cheng et al., 2022)	0.576	0.253	0.591	0.039	0.268	0.249
	EMIP (Zhang et al., 2025)	0.587	0.269	0.598	0.033	0.281	0.254
	Ours	0.566	0.249	0.589	0.041	0.270	0.252

Table 3 Quantitative results of object detection on our CamoVid60K dataset.

Methods	F-RCNN (Ren et al., 2015)	DETR (Carion et al., 2020)	DINO (Zhang et al., 2023)	RT-DETR (Zhao et al., 2024)	Ours
$mAP \uparrow$	28.72	37.56	39.84	40.95	38.39

520 **For the zero-shot image classification task**, we tested three
 521 recent methods: CLIP (Radford et al., 2021), UniCL (Yang
 522 et al., 2022), and K-LITE (Shen et al., 2022). We used the
 523 Swin-T model for both UniCL and K-LITE (pre-trained on
 524 the ImageNet-21K dataset (Deng et al., 2009)) and the ViT-
 525 B/32 pre-trained model from OpenAI’s CLIP.

All methods were trained and tested on the same NVIDIA
 RTX 3090 GPU, except for the pre-trained models used in
 the zero-shot image classification task, where we utilized the
 pre-trained models provided by the authors. For our ablation
 studies, we utilized a small subset of the dataset to evaluate

526
527
528
529
530

531 the impact of various components, thereby facilitating a rapid
532 assessment of computational efficiency.

533 5.2 Metrics

534 Following previous methods (Cheng et al., 2022; Fan et al.,
535 2022), we evaluate pixel-level masks and bounding box using
536 the following metrics:

- 537 • MAE (MAE), which quantifies the absolute per-pixel
538 discrepancy between predictions and ground-truth masks.
- 539 • Enhanced-alignment measure (E_ϕ) Fan et al. (2018),
540 which jointly reflects pixel-wise correspondence and
541 image-level statistics; it is well suited to assessing both
542 global and local accuracy in camouflaged object detec-
543 tion. We report the mean E_ϕ in our experiments.
- 544 • S-measure (S_α) Fan et al. (2017), capturing region-aware
545 and object-aware structural similarity.
- 546 • Weighted F-measure F_β^w Margolin et al. (2014), which
547 typically offers more reliable evaluation than the conven-
548 tional F_β .
- 549 • mean Dice ($mDice$), measuring similarity between two
550 sets.
- 551 • meanIoU ($mIOU$), measuring the overlap between two
552 masks.
- 553 • mean Average Precision (mAP), is the average of the
554 AP scores across all classes, and AP is a key metric for
555 evaluating object detection models, calculated as the area
556 under the precision-recall curve for a single class (rather
557 than focusing on object proposal proxy metrics).

558 5.3 Benchmarks and Discussions

559 5.3.1 Comparison with Image-Based and Video-Based 560 Motion Segmentation Methods.

561 Table 2 compares the performance of our method with
562 other approaches. Compared to image-based methods, our
563 approach demonstrates significantly superior performance
564 due to the incorporation of temporal information. When
565 evaluated against video-based methods, our approach also
566 surpasses MG (Yang et al., 2021), which relies solely on
567 estimated optical flows as input. However, compared to the
568 recent state-of-the-art method SLT-Net (Cheng et al., 2022)
569 and EMIP (Zhang et al., 2025), our method performs worse
570 on certain metrics. This is because SLT-Net (Cheng et al.,
571 2022) excels at modeling both short-term dynamics and long-
572 term temporal consistency from videos, allowing for joint
573 optimization of motion and camouflaged object segmentation
574 through a single optimization target. While EMIP (Zhang
575 et al., 2025) utilizes intermediate features from one stream
576 as interactive prompts to incorporate additional information

Table 4 Ablation study on the impact of flow information on our method.

	no OF	raw OF	refined OF
mIoU	28.34	32.16	32.81

577 into the other stream, it simultaneously conducts camou-
578 flaged segmentation and optical flow estimation.

579 5.3.2 Comparison with Object Detection Methods.

580 As shown in Table 3, our proposed model demonstrates per-
581 formance comparable to other specialized methods, owing to
582 its dual capabilities in object detection and motion segmen-
583 tation. Specifically, our method significantly outperforms
584 conventional CNN-based methods. This advantage stems
585 from dual optimizations in the detection and segmentation
586 streams, along with the integration of additional optical
587 flow information. However, when compared to DETR-
588 like methods (Zhang et al., 2023; Carion et al., 2020),
589 our approach shows mixed results. It surpasses the stan-
590 dard DETR model (Carion et al., 2020), yet falls short
591 of DINO (Zhang et al., 2023) and RT-DETR (Zhao et
592 al., 2024), advanced variants of DETR. DINO (Zhang et
593 al., 2023) enhances performance through several innova-
594 tive techniques: it employs contrastive denoising training to
595 refine one-to-one matching, a mixed query selection method
596 to better initialize the queries, and a ‘look forward twice’
597 method that utilizes gradients from subsequent layers to
598 adjust parameters more accurately. RT-DETR (Zhao et al.,
599 2024) introduces two main improvements: a hybrid encoder
600 that efficiently handles multiscale features, and a query selec-
601 tion method that reduces uncertainty, enhancing the quality
602 of the initial object queries.

603 5.3.3 Additional Analysis and Discussions.

604 As shown in Table 4, optical flow plays a crucial role in
605 the motion segmentation of camouflaged animals. By ana-
606 lyzing the motion vectors between frames, optical flow can
607 detect subtle movements, distinguishing moving animals
608 from static backgrounds. This capability is particularly useful
609 in identifying the slight movements of camouflaged animals.

610 State-of-the-art methods, including foundation models
611 trained on large datasets such as CLIP (Radford et al., 2021),
612 UniCL (Yang et al., 2022), and K-LITE (Shen et al., 2022),
613 struggle with zero-shot image classification of camouflaged
614 animals, as shown in Table 5. This is due to the subtle and
615 complex patterns of camouflaged animals, the lack of specific
616 training data, and the difficulty in generalizing across differ-
617 ent backgrounds and lighting conditions. Improving these
618 methods involves curating specialized training data (or fine-

Table 5 Zero-shot Image Classification performance on our CamoVid60K dataset.

	CLIP (Radford et al., 2021)	UniCL (Yang et al., 2022)	K-LITE (Shen et al., 2022)
mAcc	30.06	30.89	31.44

619 tuning on our dataset), using enhanced techniques like data
620 augmentation, few-shot learning, and developing context-
621 aware models.

622 6 Conclusion

623 In this paper, we introduced **CamoVid60K**, a large-scale
624 video dataset for camouflaged animal understanding, aim-
625 ing to foster further research on camouflaged animals. This
626 dataset provides a significant benchmark for camouflaged
627 animal video understanding tasks, enabling the evaluation of
628 various algorithms and methods. We also plan to scale up
629 our dataset and utilize it to build foundational models for
630 studying camouflaged animals.

631 6.1 Limitations and Future Work.

632 As mentioned in Section 3, the annotation quality in some
633 cases is suboptimal. We plan to enhance these annota-
634 tions and introduce more types of annotations in the future.
635 Additionally, our current pipeline requires images and pre-
636 computed optical flow as inputs, which restricts the genera-
637 tion of new data due to the necessity of pre-computed optical
638 flow. To address this limitation, we will propose a learnable
639 module to estimate the implicit optical flow field.

640 6.2 New Benchmark.

641 Our **CamoVid60K** dataset is a diverse and comprehensive
642 benchmark curated from publicly accessible datasets and the
643 internet to enhance the assessment and exploration of camou-
644 flaged animal understanding. It includes various camouflaged
645 animals across different environments, providing a robust
646 framework for testing and developing new models.

647 6.3 Impact on Animal Studies.

648 By providing detailed and varied data on camouflaged ani-
649 mals, the **CamoVid60K** dataset significantly contributes to
650 studying animal behavior, ecology, and evolution. Researchers
651 can utilize this dataset to explore how different species
652 employ camouflage in their natural habitats, leading to deeper
653 insights into predator-prey interactions and survival strate-
654 gies. Furthermore, this dataset can aid conservation efforts
655 by improving the detection and monitoring of endangered
656 species in their natural environments (Beery et al., 2018;

Norouzzadeh et al., 2018; Simões et al., 2023; Troscianko et al., 2017).

659 6.4 Broader Impact.

660 The study of camouflaged objects has several important
661 applications, such as identifying and safeguarding rare ani-
662 mal species, preventing wildlife trafficking, detecting med-
663 ical conditions like polyps or lung infections, and aiding
664 in search-and-rescue operations. Our dataset deliberately
665 excludes any military or sensitive scenes, ensuring its focus
666 remains on benign and beneficial applications. Besides the
667 significant applications mentioned, our work advances the
668 understanding of video content in the presence of distorted
669 motion information, contributing to the broader field of video
670 analysis and computer vision.

671 6.5 Licenses.

672 We built our dataset from previous datasets and crawled
673 online videos. Therefore, we will follow their Terms of Use
674 or Licenses (**MoCA**, **MVK**) for our dataset, which is under
675 the **CC-BY-4.0** license. The copyright remains with the origi-
676 nal owners of the videos. In addition, the dataset shall be used
677 only for non-commercial research and educational purposes.

678 A CamoVid60K Datasheet

679 Motivation

680 **For what purpose was the dataset created?** Was there a
681 specific task in mind? Was there a specific gap that needed
682 to be filled? Please provide a description.

683 There are some studies about camouflaged animal segmen-
684 tation, and most of them are image-based methods. While
685 some prior works have proposed video datasets for camou-
686 flaged animal understanding, they have only provided a small
687 amount of data with limited annotation types. To address
688 those challenges and promote more studies on biological
689 monitoring and understanding of animals' behavior, we intro-
690 duce our CamoVid60K dataset and related benchmarks for a
691 broad range of video understanding tasks. Please see Section
692 3 and Section 5 in the main paper for more details.

693 **Who created this dataset (e.g. which team, research**
694 **group) and on behalf of which entity (e.g. company, insti-**
695 **tution, organization)?**

696 The authors created the dataset from the XXX and YYY Insti- 748
 697 tutions. The authors created it for the public at large without 749
 698 reference to any particular organization or institution. 750

699 **Composition** 751

700 **What do the instances that comprise the dataset repre- 752
 701 sent (e.g. documents, photos, people, countries)? Are there 753
 702 multiple types of instances (e.g. movies, users, and ratings; 754
 703 people and interactions between them; nodes and edges)? 755
 704 Please provide a description. 756**

705 Each instance in the dataset represents a sequence of 757
 706 extracted frames from a video with different annotations 758
 707 (category, bounding box, mask, motion type, pseudo-label 759
 708 optical flow, and three referring expressions. 760

709 **How many instances are there in total (of each type, if 762
 710 appropriate)?**

711 CamoVid60K has a total of 218 instances, each containing 763
 712 frames, an associated bounding box, a mask, a motion type, 764
 713 pseudo-label optical flow, one category, and three referring 765
 714 expressions. You can see further statistics on the whole data 766
 715 in Section 3 of the main paper.

716 **Does the dataset contain all possible instances, or is it 769
 717 a sample (not necessarily random) of instances from a 770
 718 larger set? If the dataset is a sample, then what is the 771
 719 larger set? Is the sample representative of the larger 772
 720 set (e.g. geographic coverage)? If so, please describe how 773
 721 this representativeness was validated/verified. If it is not 774
 722 representative of the larger set, please describe why not 775
 723 (e.g. to cover a more diverse range of instances because 776
 724 instances were withheld or unavailable).**

725 The dataset contains all instances from previous datasets with 777
 726 additional new data that are crawled from the internet to pro- 778
 727 vide a larger volume of data with more frequent annotations 779
 728 and types, and cover a wider variety of species, ranging from 780
 729 flying to terrestrial and aquatic animals. The detailed statis- 781
 730 tics are shown in Table 1 and Section 3 of the main paper.

731 **What data does each instance consist of? "Raw" data 782
 732 (e.g. unprocessed text or images) or features? In either 783
 733 case, please provide a description. 784**

734 Each instance in our dataset comprises raw MP4 video data, 785
 735 captured at 24-30 frames per second and with resolution from 786
 736 480×360 to 3840×2160.

737 **Is there a label or target associated with each instance?If 787
 738 so, please provide a description. 788**

739 Each instance is associated with a bounding box, mask, 789
 740 motion type, pseudo-label optical flow, one category, and 790
 741 three referring expressions. 791

742 **Is any information missing from individual instances?If 792
 743 so, please provide a description, explaining why this infor- 793
 744 mation is missing (e.g., because it was unavailable). This 794
 745 does not include intentionally removed information but 795
 746 might include, e.g. redacted text. 796**

747 All instances are complete. 797

**Are relationships between individual instances made 748
 explicit (e.g. users' movie ratings, social network links)?If 749
 so, please describe how these relationships are made explicit. 750
 Some instances may have the same category name and simi- 751
 lar referring expressions because they belong to the same 752
 category. However, each instance will have its unique ID. 753**

**Are there recommended data splits (e.g. training, develop- 754
 ment/validation, testing)?If so, please provide a description 755
 of these splits, explaining the rationale behind them. 756**

CamoVid60K is explicitly designed for learning both small 757
 and large motion displacement of camouflaged animals. 758
 Therefore, it is split into two subsets: small displacement 759
 (every single frame) and large displacement (every 5 frames). 760
 This division is beneficial for evaluating motion segmenta- 761
 tion methods, as it provides a robust framework for analyzing 762
 algorithms' performance under varying motion and displac- 763
 ement conditions. Each subset will include training (168 764
 instances) and testing sets (50 instances), as mentioned 765
 in Section 3.2 of the main paper.

**Are there any errors, sources of noise, or redundancies 767
 in the dataset?If so, please provide a description. 768**

The dataset was carefully manually curated to mitigate any 769
 errors within the questions and answers. However, due to the 770
 nature and characteristics of camouflaged animals and their 771
 resolution, some frames will contain errors/mislabeling at 772
 the boundary between the animals and the background. We 773
 will keep improving the quality of the mask annotations in 774
 the next version. 775

**Is the dataset self-contained, or does it link to or other- 776
 wise rely on external resources (e.g. websites, tweets, other 777
 datasets)?If it links to or relies on external resources, a) are 778
 there guarantees that they will exist, and remain constant, 779
 over time; b) are there official archival versions of the com- 780
 plete dataset (i.e. including the external resources as they 781
 existed at the time the dataset was created); c) are there 782
 any restrictions (e.g. licenses, fees) associated with any of 783
 the external resources that might apply to a future user? 784
 Please provide descriptions of all external resources and 785
 any restrictions associated with them, as well as links or 786
 other access points, as appropriate. 787**

Entirety of the dataset will be made publicly available at our 788
[CamoVid60K website](#) (we will update our website later). 789
 CamoVid60K will be publicly released under the [CC-BY-4.0](#) 790
 license, which allows public use of the video and annotation 791
 data for both research and commercial purposes. 792

**Does the dataset contain data that might be considered 793
 confidential (e.g. data that is protected by legal privilege 794
 or by doctor-patient confidentiality, data that includes the 795
 content of individuals' non-public communications)?If 796
 so, please provide a description. 797**

No 798

799 **Does the dataset contain data that, if viewed directly,**
800 **might be offensive, insulting, threatening, or might oth-**
801 **erwise cause anxiety?**If so, please describe why.

802 No

803 **Does the dataset relate to people?**If not, you may skip the
804 remaining questions in this section.

805 No, CamoVid60K only contains animals.

806 **Does the dataset identify any subpopulations (e.g. by age,**
807 **gender)?**If so, please describe how these subpopulations are
808 identified and provide a description of their respective distri-
809 butions within the dataset.

810 No

811 **Is it possible to identify individuals (i.e. one or more**
812 **natural persons), either directly or indirectly (i.e. in com-**
813 **bination with other data) from the dataset? If so, please**
814 **describe how.**

815 No

816 **Does the dataset contain data that might be considered**
817 **sensitive in any way (e.g. data that reveals racial or ethn-**
818 **ic origins, sexual orientations, religious beliefs, political**
819 **opinions or union memberships, or locations; financial**
820 **or health data; biometric or genetic data; forms of gov-**
821 **ernment identification, such as social security numbers;**
822 **criminal history)? If so, please provide a description.**

823 No

824 **CollectionProcess**

825 **How was the data associated with each instance acquired?**
826 **Was the data directly observable (e.g. raw text, movie**
827 **ratings), reported by subjects (e.g. survey responses), or**
828 **indirectly inferred/derived from other data (e.g. part-**
829 **of-speech tags, model-based guesses for age or lan-**
830 **guage)? If data was reported by subjects or indirectly**
831 **inferred/derived from other data, was the data vali-**
832 **dated/verified? If so, please describe how.**

833 The raw video data, which is directly observable, was pro-
834 cured from the publicly accessible datasets (Camouflaged
835 Animals Dataset (CAD) (Pia Bideau, 2016), Moving Cam-
836ouflaged Animals (MoCA) (Lamdouar et al., 2020), MoCA-
837Mask (Cheng et al., 2022), Marine Video Kit (MVK) (Truong
838et al., 2023) and crawled video from internet) as shown
839in Table 1 and Section 3 in the main paper. We utilized an
840annotation tool from (Zheng et al., 2023), which is heav-
841ily based on Segment Anything Model (SAM) (Kirillov et
842al., 2023) for mask initialization and bounding box, and
843XMem (Cheng & Schwing, 2022) for mask and bounding box
844propagation. We utilized the RAFT method (Teed & Deng,
8452020) to produce an accurate estimated optical flow and
846refined it using Algorithm 1. To construct referring expres-
847sion annotations, we utilized GPT-4V (xxxx, 2023) to create
848a concise description for flying and terrestrial animals, and
849MarineGPT (Zheng et al., 2023) for aquatic animals.

850 **What mechanisms or procedures were used to collect the**
851 **data (e.g. hardware apparatus or sensor, manual human**
852 **curation, software program, software API)? How were**
853 **these mechanisms or procedures validated?**

854 The videos were downloaded in accordance with the official
855 guidelines for data access of other datasets. For additional
856 videos, we manually curated from the internet. See Section
857 3 in the main paper for a more detailed explanation.

858 **If the dataset is a sample from a larger set, what was the**
859 **sampling strategy (e.g. deterministic, probabilistic with**
860 **specific sampling probabilities)?**

861 We used all samples from the published datasets. So, there
862 is no sampling strategy.

863 **Who was involved in the data collection process**
864 **(e.g. students, crowd-workers, contractors) and how were**
865 **they compensated (e.g. how much were crowd-workers**
866 **paid)?**

867 The authors were involved in the data collection process.
868 No crowd-workers were involved during the data collection
869 process.

870 **Over what timeframe was the data collected? Does this**
871 **timeframe match the creation timeframe of the data asso-**
872 **ciated with the instances (e.g. recent crawl of old news**
873 **articles)? If not, please describe the timeframe in which**
874 **the data associated with the instances was created.**

875 The original videos within the published datasets were col-
876 lected across various occasions spanning from 2011 to 2022.
877 As for the CamoVid60K, the new videos were collected over
878 several sprints during the first half of 2024.

879 **Were any ethical review processes conducted (e.g. by**
880 **an institutional review board)? If so, please provide a**
881 **description of these review processes, including the out-**
882 **comes, as well as a link or other access point to any**
883 **supporting documentation.**

884 No

885 **Does the dataset relate to people? If not, you may skip the**
886 **remaining questions in this section.**

887 No

888 **Did you collect the data from the individuals in question**
889 **directly or obtain it via third parties or other sources**
890 **(e.g. websites)?**

891 NA

892 **Were the individuals in question notified about the data**
893 **collection? If so, please describe (or show with screen-**
894 **shots or other information) how notice was provided, and**
895 **provide a link or other access point to, or otherwise repro-**
896 **duce, the exact language of the notification itself.**

897 NA

898 **Did the individuals in question consent to the collection**
899 **and use of their data? If so, please describe (or show**
900 **with screenshots or other information) how consent was**
901 **requested and provided, and provide a link or other**

902 access point to, or otherwise reproduce, the exact lan-
903 guage to which the individuals consented.

904 NA

905 **If consent was obtained, were the consenting individu-**
906 **als provided with a mechanism to revoke their consent**
907 **in the future or for certain uses? If so, please provide a**
908 **description, as well as a link or other access point to the**
909 **mechanism (if appropriate).**

910 NA

911 **Has an analysis of the potential impact of the dataset and**
912 **its use on data subjects (e.g. a data protection impact anal-**
913 **ysis) been conducted? If so, please provide a description**
914 **of this analysis, including the outcomes, as well as a link**
915 **or other access point to any supporting documentation.**

916 NA

917 **Preprocessing/cleaning/labeling**

918 **Was any preprocessing/cleaning/labeling of the data done**
919 **(e.g. discretization or bucketing, tokenization, part-of-**
920 **speech tagging, SIFT feature extraction, removal of**
921 **instances, processing of missing values)? If so, please pro-**
922 **vide a description. If not, you may skip the remainder of**
923 **the questions in this section.**

924 There was no preprocessing done on the videos, and we only
925 did the frame extraction from the videos.

926 **Was the "raw" data saved in addition to the prepro-**
927 **cessed/cleaned/labeled data (e.g. to support unanticipated**
928 **future uses)? If so, please provide a link or other access**
929 **point to the "raw" data.**

930 The raw data in our CamoVid60K dataset is video. How-
931 ever, all methods will extract videos into frames, so we only
932 provide the extracted frames in our CamoVid60K dataset.

933 **Is the software used to preprocess/clean/label the instances**
934 **available? If so, please provide a link or other access point.**

935 We used the FFmpeg library to extract the frames. The pack-
936 ages, executable files, and sources for Windows, macOS,
937 Linux, or building from source are available on their [offi-](#)
938 [cial website](#).

939 **Distribution**

940 **Will the dataset be distributed to third parties outside**
941 **of the entity (e.g. company, institution, organization) on**
942 **behalf of which the dataset was created? If so, please pro-**
943 **vide a description.**

944 The dataset will be made publicly available and can be used
945 for non-commercial research and educational purposes under
946 the [CC-BY-4.0](#) license.

947 **How will the dataset be distributed (e.g. tarball on web-**
948 **site, API, GitHub) Does the dataset have a digital object**
949 **identifier (DOI)?**

950 The dataset will be distributed at our [CamodVid60K web-](#)
951 [site](#) (we will update our website later) upon acceptance to
952 preserve anonymization.

When will the dataset be distributed?

The complete dataset will be made available upon the accep-
tance of the paper before the camera-ready deadline.

Will the dataset be distributed under a copyright or other
intellectual property (IP) license, and/or under applica-
ble terms of use (ToU)? If so, please describe this license
and/or ToU, and provide a link or other access point to,
or otherwise reproduce, any relevant licensing terms or
ToU, as well as any fees associated with these restrictions.

CamoVid60K dataset will be publicly released under the
[CC-BY-4.0](#) license, which allows direct public use of
the video/frames and annotation data for non-commercial
research and educational purposes.

Have any third parties imposed IP-based or other restric-
tions on the data associated with the instances? If so,
please describe these restrictions and provide a link or
other access point to, or otherwise reproduce, any rele-
vant licensing terms, as well as any fees associated with
these restrictions.

No

Do any export controls or other regulatory restrictions
apply to the dataset or to individual instances? If so,
please describe these restrictions and provide a link or
other access point to, or otherwise reproduce, any sup-
porting documentation.

No

Maintenance

Who will be supporting/hosting/maintaining the dataset?

The authors of the paper will be maintaining the dataset,
pointers to which will be hosted on our [CamodVid60K](#)
[website](#) (we will update our website later), along with the
guidelines for download and preprocessing if needed.

How can the owner/curator/manager of the dataset be
contacted (e.g. email address)?

We will post the contact information on our website, primar-
ily contact through email.

Is there an erratum? If so, please provide a link or other
access point.

In the future, we will host an erratum on our [Camod-](#)
[Vid60K website](#) (we will update our website later) to host
any approved errata suggested by the authors or the video
research community.

Will the dataset be updated (e.g. to correct labeling errors,
add new instances, delete instances)? If so, please describe
how often, by whom, and how updates will be communi-
cated to users (e.g. mailing list, GitHub)?

Yes, we plan to host an erratum publicly. There are no spe-
cific plans for a v2 version, but there seem to be plenty
of opportunities for exciting future dataset work based on
CamoVid60K.

If the dataset relates to people, are there applicable limits
on the retention of the data associated with the instances

(e.g. were individuals in question told that their data would be retained for a fixed period of time and then deleted)? If so, please describe these limits and explain how they will be enforced.

No.

Will older versions of the dataset continue to be supported/hosted/maintained? If so, please describe how. If not, please describe how its obsolescence will be communicated to users.

N/A There are no older versions at the current moment. All updates regarding the current version will be communicated via our website.

If others want to extend/augment/build on/contribute to the dataset, is there a mechanism for them to do so? If so, please provide a description. Will these contributions be validated/verified? If so, please describe how. If not, why not? Is there a process for communicating/distributing these contributions to other users? If so, please provide a description. Contributions will be made possible using comment functions in our [CamodVid60K website](#) (we will update our website later). The CamoVid60K team will verify any new contributions before publishing them on our website, and then we will host any approved errata suggested by the video research community.

Acknowledgements This work is supported by an internal grant from HKUST (R9429), the National Research Foundation, Singapore, and DSO National Laboratories under the AI Singapore Programme (AISG Award No: AISG2-GC-2023-008), Career Development Fund (CDF) of Agency for Science, Technology and Research (A*STAR) (No.: C233312028), National Research Foundation, Singapore and Infocomm Media Development Authority under its Trust Tech Funding Initiative (No. DTC-RGC-04). This work was partially done when Tuan Anh Vu was a research resident at CFAR & IHPC, A*STAR, Singapore.

Data Availability All data, codes, and related materials are available via our [CamodVid60K website](#).

References

- Beery, S., Van Horn, G., Perona, P.: Recognition in terra incognita. In: ECCV, pp. 456–473 (2018)
- Butler, D.J., Wulff, J., Stanley, G.B., Black, M.J.: A naturalistic open source movie for optical flow evaluation. In: ECCV (2012)
- Caron, M., Touvron, H., Misra, I., Jégou, H., Mairal, J., Bojanowski, P., Joulin, A.: Emerging properties in self-supervised vision transformers. In: ICCV (2021)
- Cheng, B., Misra, I., Schwing, A.G., Kirillov, A., Girdhar, R.: Masked-attention mask transformer for universal image segmentation. In: CVPR, pp. 1290–1299 (2022)
- Cheng, H.K., Schwing, A.G.: XMem: Long-term video object segmentation with an atkinson-shiffrin memory model. In: ECCV (2022)
- Cheng, X., Xiong, H., Fan, D.-P., Zhong, Y., Harandi, M., Drummond, T., Ge, Z.: Implicit motion handling for video camouflaged object detection. In: CVPR (2022)
- Deng, J., Dong, W., Socher, R., Li, L.-J., Li, K., Fei-Fei, L.: Imagenet: A large-scale hierarchical image database. In: CVPR, pp. 248–255 (2009)
- Dosovitskiy, A., Beyer, L., Kolesnikov, A., Weissenborn, D., Zhai, X., Unterthiner, T., Dehghani, M., Minderer, M., Heigold, G., Gelly, S., et al.: An image is worth 16x16 words: Transformers for image recognition at scale. arXiv preprint [arXiv:2010.11929](#) (2020)
- Dosovitskiy, A., Fischer, P., Ilg, E., Häusser, P., Hazırbaş, C., Golkov, V., Smagt, P., Cremers, D., Brox, T.: FlowNet: Learning optical flow with convolutional networks. In: ICCV (2015)
- Fan, D.-P., Cheng, M.-M., Liu, Y., Li, T., Borji, A.: Structure-measure: A New Way to Evaluate Foreground Maps. In: ICCV (2017)
- Fan, D.-P., Ji, G.-P., Xu, P., Cheng, M.-M., Sakaridis, C., Van Gool, L.: Advances in deep concealed scene understanding. *Visual Intelligence* (2023)
- Fan, D.-P., Ji, G.-P., Xu, P., Cheng, M.-M., Sakaridis, C., & Van Gool, L. (2023). Advances in deep concealed scene understanding. *Visual Intelligence*, 1, 1–16.
- Gebru, T., Morgenstern, J., Vecchione, B., Vaughan, J.W., Wallach, H., Iii, H.D., Crawford, K.: Datasheets for datasets. *Communications of the ACM* 64(12), 86–92 (2021)
- Gebru, T., Morgenstern, J., Vecchione, B., Vaughan, J. W., Wallach, H., Iii, H. D., & Crawford, K. (2021). Datasheets for datasets. *Communications of the ACM*, 64(12), 86–92.
- He, R., Dong, Q., Lin, J., Lau, R.W.: Weakly-supervised camouflaged object detection with scribble annotations. In: AAAI (2023)
- He, C., Li, K., Zhang, Y., Tang, L., Zhang, Y., Guo, Z., Li, X.: Camouflaged object detection with feature decomposition and edge reconstruction. In: CVPR (2023)
- He, K., Zhang, X., Ren, S., Sun, J.: Deep residual learning for image recognition. In: CVPR, pp. 770–778 (2016)
- Ji, G.-P., Fan, D.-P., Chou, Y.-C., Dai, D., Liniger, A., Van Gool, L.: Deep gradient learning for efficient camouflaged object detection. *MIR* (2023)
- Ji, P., Zhong, Y., Li, H., Salzmann, M.: Null space clustering with applications to motion segmentation and face clustering. In: ICIP, pp. 283–287 (2014)
- Ji, G.-P., Fan, D.-P., Chou, Y.-C., Dai, D., Liniger, A., & Van Gool, L. (2023). Deep gradient learning for efficient camouflaged object detection. *Machine Intelligence Research*, 20, 92–108.
- Kowal, M., Siam, M., Islam, M.A., Bruce, N.D., Wildes, R.P., Derpanis, K.G.: A deeper dive into what deep spatiotemporal networks encode: Quantifying static vs. dynamic information. In: CVPR (2022)
- Lamdouar, H., Xie, W., Zisserman, A.: Segmenting invisible moving objects. In: BMVC (2021)
- Lamdouar, H., Xie, W., Zisserman, A.: The making and breaking of camouflage. In: ICCV, pp. 832–842 (2023)
- Lamdouar, H., Yang, C., Xie, W., Zisserman, A.: Betrayed by motion: Camouflaged object discovery via motion segmentation. *ACCV* (2020)
- Le, T.-N., Nguyen, T.V., Nie, Z., Tran, M.-T., Sugimoto, A.: Anabranch network for camouflaged object segmentation. *CVIU* (2019)
- Le, T.-N., Cao, Y., Nguyen, T.-C., Le, M.-Q., Nguyen, K.-D., Do, T.-T., Tran, M.-T., & Nguyen, T. V. (2021). Camouflaged instance segmentation in-the-wild: Dataset, method, and benchmark suite. *IEEE Transactions on Image Processing*, 31, 287–300.
- Lin, T.-Y., Maire, M., Belongie, S., Hays, J., Perona, P., Ramanan, D., Dollár, P., Zitnick, C.L.: Microsoft COCO: Common objects in context. In: ECCV, pp. 740–755 (2014). Springer
- Lv, Y., Zhang, J., Dai, Y., Li, A., Liu, B., Barnes, N., Fan, D.-P.: Simultaneously localize, segment and rank the camouflaged objects. In: CVPR (2021)
- Margolin, R., Zelnik-Manor, L., Tal, A.: How to evaluate foreground maps? In: CVPR (2014)
- Mayer, N., Ilg, E., Häusser, P., Fischer, P., Cremers, D., Dosovitskiy, A., Brox, T.: A large dataset to train convolutional networks for disparity, optical flow, and scene flow estimation. In: *IEEE Inter-*

- national Conference on Computer Vision and Pattern Recognition (CVPR) (2016)
- 1125 Menze, M., Geiger, A.: Object scene flow for autonomous vehicles. In: CVPR (2015)
- 1126 Meunier, E., Badoual, A., Boutheymy, P.: Em-driven unsupervised learning for efficient motion segmentation. *IEEE T-PAMI* (2022)
- 1127 Meunier, E., Badoual, A., & Boutheymy, P. (2022). Em-driven unsupervised learning for efficient motion segmentation. *IEEE Transactions on Pattern Analysis and Machine Intelligence*, 45, 4462–4473.
- 1128 Norouzzadeh, M.S., Nguyen, A., Kosmala, M., Swanson, A., Palmer, M.S., Packer, C., Clune, J.: Automatically identifying, counting, and describing wild animals in camera-trap images with deep learning. *PNAS* 115(25), 5716–5725 (2018)
- 1129 Norouzzadeh, M. S., Nguyen, A., Kosmala, M., Swanson, A., Palmer, M. S., Packer, C., & Clune, J. (2018). Automatically identifying, counting, and describing wild animals in camera-trap images with deep learning. *PNAS*, 115(25), 5716–5725.
- 1130 OpenAI, t.: GPT-4 technical report. arXiv preprint [arXiv:2303.08774](https://arxiv.org/abs/2303.08774) (2023)
- 1131 Oquab, M., Darcet, T., Moutakanni, T., Vo, H.V., Szafraniec, M., Khalidov, V., Fernandez, P., HAZIZA, D., Massa, F., El-Nouby, A., Assran, M., Ballas, N., Galuba, W., Howes, R., Huang, P.-Y., Li, S.-W., Misra, I., Rabbat, M., Sharma, V., Synnaeve, G., Xu, H., Jegou, H., Mairal, J., Labatut, P., Joulin, A., Bojanowski, P.: DINOv2: Learning robust visual features without supervision. *TMLR* (2024)
- 1132 Pei, J., Cheng, T., Fan, D.-P., Tang, H., Chen, C., Van Gool, L.: Osformer: One-stage camouflaged instance segmentation with transformers. In: *ECCV* (2022)
- 1133 Pia Bideau, E.L.-M.: It's moving! a probabilistic model for causal motion segmentation in moving camera videos. In: *ECCV* (2016)
- 1134 Radford, A., Kim, J.W., Hallacy, C., Ramesh, A., Goh, G., Agarwal, S., Sastry, G., Askell, A., Mishkin, P., Clark, J., Krueger, G., Sutskever, I.: Learning transferable visual models from natural language supervision. In: *ICML*, pp. 8748–8763 (2021)
- 1135 Rands, M.R., Adams, W.M., Bennun, L., Butchart, S.H., Clements, A., Coomes, D., Entwistle, A., Hodge, I., Kapos, V., Scharlemann, J.P., and others: Biodiversity conservation: challenges beyond 2010. *Science* 329(5997), 1298–1303 (2010)
- 1136 Ren, S., He, K., Girshick, R., Sun, J.: Faster R-CNN: Towards real-time object detection with region proposal networks. *NeurIPS* 28 (2015)
- 1137 Seo, S., Lee, J.-Y., Han, B.: Urvos: Unified referring video object segmentation network with a large-scale benchmark. In: *ECCV*, pp. 208–223 (2020). Springer
- 1138 Shao, S., Li, Z., Zhang, T., Peng, C., Yu, G., Zhang, X., Li, J., Sun, J.: Objects365: A large-scale, high-quality dataset for object detection. In: *ICCV*, pp. 8430–8439 (2019)
- 1139 Shen, S., Li, C., Hu, X., Xie, Y., Yang, J., Zhang, P., Gan, Z., Wang, L., Yuan, L., Liu, C., and others: K-lite: Learning transferable visual models with external knowledge. *NeurIPS* 35, 15558–15573 (2022)
- 1140 Simões, F., Bouveyron, C., Precioso, F.: Deepwild: Wildlife identification, localisation and estimation on camera trap videos using deep learning. *Ecological Informatics* 75, 102095 (2023)
- 1141 Simões, F., Bouveyron, C., & Precioso, F. (2023). Deepwild: Wildlife identification, localisation and estimation on camera trap videos using deep learning. *Ecological Informatics*, 75, Article 102095.
- 1142 Soofi, M., Sharma, S., Safaei-Mahroo, B., Sohrabi, M., Organli, M.G., Waltert, M.: Lichens and animal camouflage: some observations from central asian ecoregions. *Journal of Threatened Taxa* 14(2), 20672–20676 (2022)
- 1143 Soofi, M., Sharma, S., Safaei-Mahroo, B., Sohrabi, M., Organli, M. G., & Waltert, M. (2022). Lichens and animal camouflage: some observations from central asian ecoregions. *Journal of Threatened Taxa*, 14(2), 20672–20676.
- 1144 Sun, G., An, Z., Liu, Y., Liu, C., Sakaridis, C., Fan, D.-P., Van Gool, L.: Indiscernible object counting in underwater scenes. In: *CVPR* (2023)
- 1145 Teed, Z., Deng, J.: RAFT: Recurrent all-pairs field transforms for optical flow. In: *ECCV* (2020)
- 1146 Troscianko, J., Skelhorn, J., Stevens, M.: Quantifying camouflage: how to predict detectability from appearance. *BMC Evolutionary Biology* 17, 1–13 (2017)
- 1147 Troscianko, J., Skelhorn, J., & Stevens, M. (2017). Quantifying camouflage: how to predict detectability from appearance. *BMC Evolutionary Biology*, 17, 1–13.
- 1148 Truong, Q.-T., Vu, T.-A., Ha, T.-S., Lokoč, J., Tim, Y.H.W., Joneja, A., Yeung, S.-K.: Marine Video Kit: A new marine video dataset for content-based analysis and retrieval. In: *MMM*. Springer, ??? (2023)
- 1149 Vu, T.-A., Nguyen, D.T., Guo, Q., Hua, B.-S., Chung, N.M., Tsang, I.W., Yeung, S.-K.: Leveraging open-vocabulary diffusion to camouflaged instance segmentation. arXiv preprint [arXiv:2312.17505](https://arxiv.org/abs/2312.17505) (2023)
- 1150 Wang, Q., Chang, Y.-Y., Cai, R., Li, Z., Hariharan, B., Holynski, A., Snavely, N.: Tracking everything everywhere all at once. In: *ICCV* (2023)
- 1151 Wang, F., Cao, P., Li, F., Wang, X., He, B., & Sun, F. (2022). Watb: Wild animal tracking benchmark. *International Journal of Computer Vision*, 131(4), 899–917. <https://doi.org/10.1007/s11263-022-01732-3>
- 1152 Xie, C., Xiang, Y., Harchaoui, Z., Fox, D.: Object discovery in videos as foreground motion clustering. In: *CVPR* (2019)
- 1153 Xie, J., Xie, W., Zisserman, A.: Segmenting moving objects via an object-centric layered representation. *NeurIPS* (2022)
- 1154 Xie, J., Xie, W., & Zisserman, A. (2022). Segmenting moving objects via an object-centric layered representation. *Advances in neural information processing systems*, 35, 28023–28036.
- 1155 Yang, C., Lamdouar, H., Lu, E., Zisserman, A., Xie, W.: Self-supervised video object segmentation by motion grouping. In: *ICCV* (2021)
- 1156 Yang, J., Li, C., Zhang, P., Xiao, B., Liu, C., Yuan, L., Gao, J.: Unified contrastive learning in image-text-label space. In: *CVPR*, pp. 19163–19173 (2022)
- 1157 Yang, Z., Wang, J., Ye, X., Tang, Y., Chen, K., Zhao, H., Torr, P.S.: Language-aware vision transformer for referring segmentation. *IEEE T-PAMI* 00(00), 1–18 (2024)
- 1158 Zeng, Y., Zhang, P., Zhang, J., Lin, Z., Lu, H.: Towards high-resolution salient object detection. In: *ICCV*, pp. 7234–7243 (2019)
- 1159 Zhang, L., Gao, J., Xiao, Z., Fan, H.: Animaltrack: A benchmark for multi-animal tracking in the wild. *International Journal of Computer Vision* 131(2), 496–513 (2022) <https://doi.org/10.1007/s11263-022-01711-8>
- 1160 Zhang, H., Li, F., Liu, S., Zhang, L., Su, H., Zhu, J., Ni, L., Shum, H.-Y.: DINO: DETR with improved denoising anchor boxes for end-to-end object detection. In: *ICLR* (2023)
- 1161 Zhang, L., Gao, J., Xiao, Z., & Fan, H. (2022). Animaltrack: A benchmark for multi-animal tracking in the wild. *International Journal of Computer Vision*, 131(2), 496–513. <https://doi.org/10.1007/s11263-022-01711-8>
- 1162 Zhang, X., Xiao, T., Ji, G.-P., Wu, X., Fu, K., & Zhao, Q. (2025). Explicit motion handling and interactive prompting for video camouflaged object detection. *IEEE Transactions on Image Processing*, 34, 2853–2866.
- 1163 Zhao, Y., Lv, W., Xu, S., Wei, J., Wang, G., Dang, Q., Liu, Y., Chen, J.: Detsr beat yolos on real-time object detection. In: *Proceedings of the IEEE/CVF Conference on Computer Vision and Pattern Recognition (CVPR)*, pp. 16965–16974 (2024)
- 1164 Zheng, Z., Xie, Y., Liang, H., Yu, Z., Yeung, S.-K.: CoralVOS: Dataset and benchmark for coral video segmentation. arXiv preprint [arXiv:2310.01946](https://arxiv.org/abs/2310.01946) (2023)

- 1255 Zheng, Z., Zhang, J., Vu, T.-A., Diao, S., Tim, Y.H.W., Yeung, S.-
1256 K.: MarineGPT: Unlocking secrets of ocean to the public. arXiv
1257 preprint [arXiv:2310.13596](https://arxiv.org/abs/2310.13596) (2023)
- 1258 Zhou, B., Zhao, H., Puig, X., Fidler, S., Barriuso, A., Torralba, A.: Scene
1259 parsing through ade20k dataset. In: CVPR, pp. 633–641 (2017)

Publisher's Note Springer Nature remains neutral with regard to juris- 1260
1261 dictional claims in published maps and institutional affiliations.

Springer Nature or its licensor (e.g. a society or other partner) holds
exclusive rights to this article under a publishing agreement with the
author(s) or other rightsholder(s); author self-archiving of the accepted
manuscript version of this article is solely governed by the terms of such
publishing agreement and applicable law.